Published in final edited form as:
Hear Res. 2009 November ; 257(1-2): 41–52. doi:10.1016/j.heares.2009.07.010.

Hemispheric Asymmetry in Mid and Long Latency Neuromagnetic Responses to Single Clicks

Mary F. Howard[a] and **David Poeppel**[a,b,c]

[a] Department of Linguistics, University of Maryland, 1401 Marie Mount Hall, College Park, MD 20742-7505, USA

[b] Department of Biology, University of Maryland, 1210 Biology-Psychology Building, College Park, MD 20742, USA

[c] Department of Psychology, New York University, 6 Washington Place, New York, NY 10003, USA

Abstract

We examine lateralization in the evoked magnetic field response to a click stimulus, observing that lateralization effects previously demonstrated for tones, noise, frequency modulated sweeps and certain syllables are also observed for (acoustically simpler) clicks. These effects include a difference in the peak latency of the M100 component of the evoked field waveform such that the peak consistently appears earlier in the right hemisphere, as well as rightward lateralization of field amplitude during the rise of the M100 component. Our review of previous findings on M100 lateralization, taken together with our data on the click-evoked response, leads to the hypothesis that these lateralization effects are elicited by stimuli containing a sharp sound energy onset or acoustic transition rather than specific types of stimuli. We argue that both the latency and the amplitude lateralization effects have a common origin, namely, hemispheric asymmetry in the amplitude of the magnetic field generated by one or more sources active during the M100 rise. While anatomical asymmetry cannot be excluded as the cause of the amplitude difference, we propose that the difference reflects a rightward asymmetry in the processing of sound energy onsets that potentially underlies the lateralization of several functions.

Keywords

Auditory; Evoked field; M100; N1m; Lateralization; MEG

INTRODUCTION

Determining the neural basis of hemispheric differences in auditory processing is crucial to the formulation of a biologically-based theory of speech lateralization. However, the discovery of neurobiological asymmetries potentially related to functional lateralization effects and the explication of *causal* relationships linking the asymmetries to such effects is quite difficult. One method of attacking the problem is to use magnetoencephalography (MEG), which allows the magnetic field response evoked by auditory signals to be measured for the individual

Corresponding author: Mary F. Howard, University of Maryland, Biology-Psychology Bldg. #3263, College Park, MD 20742, Tel.: 301 405 2587, 301 908 4942, Fax: 301 405 7104, Mary F. Howard mfhoward@umd.edu, David Poeppel david.poeppel@nyu.edu.

hemispheres with very high sensitivity. Neurobiological asymmetries become evident with this methodology because they produce hemispheric differences, that is, lateralization, in various attributes of the magnetic field response. The temporal resolution of MEG makes it possible to determine the timing of identified differences with a high degree of precision, thus constraining the potential sources of asymmetric activity in the temporal dimension.

In this study, we seek to characterize lateralization in the magnetic field response evoked by a simple, single click stimulus by identifying statistically significant effects that are consistently present across two separate experiments. We especially wish to determine if two potentially related lateralization effects, previously observed in the M100 component[1] of the response evoked by other auditory stimuli, are present in the response to the click. These effects include hemispheric asymmetry in the latency of the M100 peak and in magnetic field amplitude during the M100 rise. An earlier M100 peak has been observed in the right hemisphere for a variety of stimuli, including tones (Gabriel, et al., 2004;Huotilainen, et al., 1998;Jin, et al., 2007;Kanno, et al., 2000;Kirveskari, et al., 2006;Pardo, et al., 1999;Roberts, et al., 2000;Rosburg, et al., 2002;Salajegheh, et al. 2004), vowels (Kirveskari, et al., 2006;Poeppel, et al., 1997) and syllables starting with a stop consonant (Gage, et al., 1998,2002;Obleser, et al., 2003). In addition, rightward lateralization of both M100 peak latency and response amplitude has been found in the magnetic field response to frequency-modulated (FM) sweeps (König, et al., 2008) and in the tangential component of the N100 electric potential response for white noise and tone stimuli (Hine & Debener, 2007). Although many, seemingly disparate stimuli appear to produce rightward lateralization in M100 peak latency, an earlier M100 peak has been observed in the left hemisphere for tones with gradual onsets (Pardo, et al., 1999). This suggests that M100 lateralization effects may be associated with onset characteristics and, indeed, the various stimuli found to elicit rightward lateralization are commonly characterized by their relatively sharp acoustic onsets. Because the onset of the click stimulus is extremely sharp, we hypothesize that its magnetic field response will exhibit significant rightward lateralization in M100 peak latency and in the amplitude of the field response during the M100 rise.

MATERIALS AND METHODS

Experiment 1

Subjects—Fourteen subjects (mean age 24.3, 8 male) took part in the experiment after providing informed consent. All were right-handed (Oldfield, 1971), reported normal hearing, and had no history of neurological disorders. On the hearing check administered prior to the experiment, all subjects perceived stimulus sound levels as comfortable and of equal loudness in both ears.

Stimuli—Eleven stimuli were generated as .wav files, 500 ms in length with a sampling frequency of 16k Hz (using Matlab 7, The Mathworks, Inc.). The stimuli consisted of single clicks (0.0625 ms square wave, positive polarity) and click pairs (two 0.0625 ms square waves, positive followed by negative polarity). For single clicks, the square wave onset was offset from stimulus time zero by 0, 20, 40, 60, 100, or 140 ms. For click pairs, the interval between square wave onsets was 20, 40, 60, 100, or 140 ms. Sound levels for all stimuli were set to ~70dB SPL.

Procedure—Stimuli were delivered binaurally through plastic tubing connected to ear pieces inserted in the ear canals of the subjects (EAR Tone 3A System), with presentation controlled

[1]Also known as the N1m, the M100 is the prominent component of the evoked field that peaks approximately 100 ms after stimulus onset.

via Presentation version 11.3 (Neurobehavioral Systems, Inc.). The eleven stimuli were presented 96 times each in pseudo-random order. The experiment was divided into 4 identical blocks, providing subjects with an opportunity to rest between blocks. In order to maintain alertness, the subjects were asked to indicate whether they heard a single click or a click pair by pressing one of two buttons on a response pad held in one hand. They were encouraged to be accurate but told that response time was not important to the results. Response-to-next stimulus intervals were set to random values between 2000 to 2125 ms, producing random ISI's of at least 2 seconds. Subjects were instructed to switch hands between blocks to balance any hand-related effects and to proceed (by a button press) with the next block when they were ready and alert.

Neuromagnetic Recording—The neuromagnetic data were acquired in a magnetically shielded room (Yokogawa, Japan) using a 160-channel, whole-head axial gradiometer system (5 cm baseline, SQUID-based sensors, KIT, Kanazawa, Japan). MEG channels included 157 head channels plus 3 reference channels that recorded the environmental magnetic field data for noise reduction purposes. Data were continuously recorded using a sampling rate of 1000 Hz, on-line ltered between 1 and 200 Hz with a notch at 60 Hz.

Data Processing—The recorded data were noise reduced off-line using the CALM algorithm (Adachi, et al., 2001). For one subject, approximately half of the recorded data had to be discarded due to noise contamination resulting from nearby construction activity. The examined MEG data for each stimulus condition covered 1000 ms epochs that included 400 ms pre-trigger and 600 ms post-trigger periods. Latency times for the processed data were adjusted for the 20 ms delay between trigger generation and the actual time of stimulus presentation. Epochs with neuromagnetic responses > 2500 fT were automatically rejected.

For this study, further analysis of the data included only those epochs representing the response to the single click stimuli (the click pair data forms the basis of a separate study). Each epoch was time shifted by its associated stimulus offset from time zero in order to align stimulus presentation times, then 860 ms of the epoch were retained for further processing (−400 ms to 460 ms). For each subject, the adjusted epoch data for each MEG channel were averaged, and the average was baseline corrected based on the 400 ms period prior to time zero to produce an estimated evoked response. The mean number of epochs included in the average for each of 13 subjects was 519 (range 492–546). For the subject with noise-contaminated data, 255 epochs were included in the average.

Experiment 2

Subjects—Nineteen subjects (average age 22.2 years, 4 male) took part in the experiment after providing informed consent. All were right-handed (Oldfield, 1971), reported normal hearing, and had no history of neurological disorders. On the hearing check administered prior to the experiment, all subjects perceived stimulus sound levels as comfortable and equal in both ears.

Stimuli—Two stimuli were generated as .wav files, 500 ms in length with a sampling frequency of 16k Hz (using Matlab 7, The Mathworks, Inc.). The stimuli consisted of a single click (0.0625 ms square wave, positive polarity) and a click pair (two 0.0625 ms square waves, positive followed by negative polarity) with a 40 ms interval separating the square wave onsets.

Procedure—The procedures were identical to those followed in Experiment 1 except that the two stimuli were presented 480 times each (in pseudo-random order) with presentation divided into 8 identical blocks

Neuromagnetic Recording—The neuromagnetic signal data were acquired as described for Experiment 1. Data were continuously recorded using a sampling rate of 1000 Hz, on-line ltered between 1 and 100 Hz with a notch at 60 Hz.

Data Processing—Recorded data were noise-reduced using the time-shift principle component analysis algorithm (TSPCA) (de Cheveigne'& Simon, 2007). The examined MEG data for each stimulus condition covered 860 ms epochs that included 400 ms pre-trigger and 460 ms post-trigger periods. Subsequent processing of the data was the same as described for Experiment 1. Further analysis of the processed data again included only those epochs representing the response to the single click stimuli. The total number of accepted epochs averaged 472 per subject (range 441–480).

Data Analysis (Experiments 1 and 2)—All analyses described in this section were based on the baseline-corrected, epoch-averaged subject data for Experiments 1 and 2 described under *Data Processing*. Because the upper limit of the on-line filtering performed during acquisition differed between Experiments 1 (200 Hz) and 2 (100 Hz), the response data for Experiment 1 subjects were low-pass filtered off-line with an upper limit of 100 Hz (21 point Hamming window) to produce MEG channel response data comparable to the data acquired on-line in Experiment 2. The MEG channel response data sets for the two experiments constituted the broad-band response data.

The portion of the evoked response comprising mainly frequencies from the lower end of the gamma band was extracted from the broad-band response data for each subject through the application of a 22–58 Hz band-pass filter (113 point Hamming window). Similarly, the slow-wave portion of the response comprising mainly sub-gamma band frequencies was extracted via a low-pass 22 Hz filter (91 point Hamming window). For the slow-wave data, root-mean-square (RMS) waveforms were computed for each subject by averaging over the set of channels restricted to either the right (74 channels) or the left (76 channels) hemisphere. The peak latencies of the M50 and M100 components in each hemisphere were found if they could be identified in the RMS waveform.

The broad-band, slow-wave and gamma-band magnetic field data sets were averaged across subjects to obtain corresponding grand average data for each of the two experiments. The grand average data were used to compute average evoked response waveforms across all channels after first setting the data for each channel to the same polarity. Uniform polarity was attained by: 1) computing the RMS waveform of the grand average response across all channels (i.e., the whole-head RMS), 2) finding the peak latency of a defined prominent component in the RMS waveform (e.g. the M100), 3) setting the grand average response for each channel to a positive polarity at the time corresponding to the latency of this peak, and 4) changing the polarity of the channel response at all other times to be consistent with this peak polarity setting.

The evoked field waveform for each hemisphere was computed by first averaging response across a channel subset restricted to the hemisphere. The restricted subset was selected to include 28 channels (7 from each quadrant) that best reflect the activation of auditory cortex (for more on channel selection, see *Results*). The resulting waveform was then offset by the value of its amplitude at latency 0 ms effectively setting the response level at the time of stimulus presentation to zero for both hemispheres. Confidence limits (95%) on all waveforms were found by bootstrap resampling of the subject data (Efron & Tibshirani, 1993). The results of the bootstrap resampling were used to determine the probability distribution of the inter-hemispheric differences in component latencies and the periods of significant inter-hemispheric differences in magnetic field response. The frequency amplitude spectra of the resampled waveforms were found by computing the fast Fourier transform (1024 point, zero-padded) from time 0–299 ms. The results were used to determine the mean frequency amplitude

spectrum and 95% confidence limits for the evoked response (first 300 ms), together with the probability distribution of inter-hemispheric differences in peak frequency, for each experiment.

Both experiments were conducted in accordance with the Institutional Review Board of the University of Maryland.

RESULTS

Broad-Band Response Components

Prior to the analysis of lateralization in the grand average evoked response, channel polarity was reset to be consistent across all 157 channels as described in the Methods section. The whole-head RMS waveforms used in this process, together with the individual channel response data, are shown in Figure 1a for both Experiments 1 and 2. The RMS waveform has a prominent N1m component with a peak latency of 89 ms for Experiment 1 and 91 ms for Experiment 2. For both experiments, the waveform of the broad-band response, computed by averaging across all 157 channels (Figure 1b), reveals that all canonical components of the auditory response are present (Eggermont & Ponton, 2002; Picton, et al., 1974), including both middle latency (N_am, P_am, N_bm, P1m/P_bm) and long latency (N1m, P2m, N2m) components. Peak latencies for all but the N2m component are quite consistent between experiments, differing by 3 ms or less. The average component latencies in milliseconds across the two experiments are: N_am - 18, P_am - 34, N_bm - 47, P1m - 58, N1m - 90, P2m - 160, N2m - 242. Also apparent in the waveforms is a slow-wave (low frequency-band) component, opposite in polarity from the N1m, which largely coincides with the middle latency components.

The topography of the surface contour map of the evoked response at the N1m peak latency is similar for both experiments and is consistent with bilateral dipole activation in the auditory cortex (Figure 1c). The stability of the spatial patterns between experiments made it possible to select a set of 28 channels, 7 in each quadrant, for which the N1m response was maximal in both experiments. This select set of channels formed the basis of all grand average computations specific to the right and left hemispheres, as well as all bootstrap resampling analyses, performed in this study.

The evoked response waveforms for the right and left hemispheres based on the select channel set are displayed in Figure 2a. The peak latencies for corresponding waveform components across experiments remain consistent with differences ≤ 6 ms observed for all components, including the N2m, and a mean difference of 2.4 ms. Variation in peak latencies between hemispheres is also minimal with the notable exception of the peak latency of the N1m component. For both experiments, latencies for all but the N1m component differed between hemispheres by 5 ms or less (mean difference, 2 ms). The N1m peak latency, however, was 9 ms earlier in the right hemisphere in both experiments. The earlier peak latency of N1m in the right hemisphere was determined to be significant for both Experiment 1 ($p < .003$) and Experiment 2 ($p < .03$) based on probability distributions for the latency difference value obtained via bootstrap resampling (4000 repetitions). The average waveforms for both hemispheres together with their 95% confidence limits based on the bootstrap resampling results are shown in Figure 2b.

The frequency amplitude spectra (means and 95% confidence limits obtained via bootstrap resampling, 4000 repetitions) of the first 300 ms of the evoked response waveform for each experiment, computed as described in Methods, are shown in Figure 2c. The spectra indicate that the response is dominated by theta-band frequencies with peaks in mean amplitude occurring at approximately 6.7 Hz in the left and 6.1 Hz in the right hemisphere for Experiment 1 and 7.5 Hz in the left and 6.1 Hz in the right hemisphere for Experiment 2. The finding of a

lower peak frequency in the right hemisphere was not determined to be significant for either experiment although a trend toward significance was found for Experiment 2 ($p<0.1$).

Gamma-Band Response Components

The whole-head RMS waveforms (along with the individual channel responses) for the low-gamma frequency (22–58 Hz) portion of the grand average evoked responses are shown in Figure 3a. These results indicate that the evoked response in the low-gamma frequency range comprises the middle latency components. The corresponding evoked waveforms (Figure 3b), computed by resetting channel polarities based on the peak latency of the N_bm component in the RMS waveform (47 ms for Experiment 1, 46 ms for Experiment 2) clearly show the middle latency responses, with peaks that vary by no more than 1 ms across experiments. The average component peaks across the experiments are N_am - 20, P_am - 33, N_bm - 47, P1m (or P_bm) - 61, forming a transient gamma-band wave of ~36 Hz.

The topographical patterns of the transient gamma-band response at the peak latency times are consistent with the activation of auditory cortex and are very similar for the two experiments (Figure 3c). Patterns in the right and left hemispheres are highly symmetric in appearance. The waveforms for the right and left hemispheres have peak latencies for the middle latency response components that differ by no more than 3 ms. The waveforms, shown in Figure 3d, exhibit few significant hemispheric differences in response amplitude in Experiment 1 and none in Experiment 2 (based on bootstrap resampling, 4000 repetitions).

Slow-wave Response Components

The whole-head RMS waveforms (along with the individual channel responses) for the low frequency (<22 Hz) portion of the grand average evoked responses are shown in Figure 4a. The RMS waveforms have a prominent M100 component with a peak latency of 93 ms for Experiment 1 and 94 ms for Experiment 2. The waveform of the response averaged across channels (Figure 4b) displays the characteristic low-frequency band components of the auditory response including the M50, the M100, and the M150. Across experiments, M100 and M150 peak latencies exhibit minimal variation (2 ms) in contrast with the M50 peak latency, which differs by 16 ms.

The topographical patterns of the response at the peak latency times are consistent with activation of auditory cortex and are quite stable across the two experiments (Figure 4c). Patterns for the right and left hemispheres have a generally symmetric appearance, with the exception of the patterns for the earliest peak latency which indicate a strong M50 dipole activation in the left hemisphere coinciding with a transition from M50 to M100 dipole activation in the right hemisphere. The patterns at latencies of ~160 ms also display some asymmetry and appear to reflect activity from more than one source.

The waveforms for the right and left hemispheres obtained for Experiments 1 and 2 exhibit significant differences in the magnetic field response, with some differences appearing in both experiments (Figure 5a and b). Preceding the M100 peak, the magnetic field response in the direction of M100 polarity is greater in the right than in the left hemisphere. In Experiment 1, the difference was found to be significant (via bootstrap resampling, 2000 repetitions) from 49 through 74 ms with a maximum at 69 ms. In Experiment 2, the difference was found to be significant from 12 through 72 ms with a maximum at 65 ms. Together, these results indicate that there is a consistent asymmetry in the magnetic field response during the rise of the M100 component at ~49–72 ms with a maximum at ~ 67 ms.

Further evidence of asymmetry during this time is also evident in the surface topography patterns shown in Figure 5c. In both experiments, M50 dipole activation appears to persist in

the left hemisphere while M100 dipole activation appears to develop in the right hemisphere. Although the waveform and spatial patterns are very similar across experiments, M100 amplitude is greater and its emergence is earlier in Experiment 1. During the course of M100 activation, a posterior-to-anterior shift in the location of the M100 source is clearly visible in the right hemisphere in the topographical maps for both experiments.

The asymmetry evident during the M50-M100 transition is accompanied by hemispheric differences in M50 and M100 peak latencies. The earlier peak latency of the M100 component in the right hemisphere was determined to be significant for both Experiment 1 ($p < .005$) and Experiment 2 ($p < .008$) based on bootstrap resampling probability distributions for the latency difference value (4000 repetitions). The later peak latency of the M50 component in the left hemisphere was determined to be significant for Experiment 1 ($p < .015$) but not for Experiment 2 ($p < .175$). Examination of the response patterns at 65 ms for individual subjects revealed that only one subject (from Experiment 2) exhibited a pattern completely reversed from the average, that is, M50 dipole activation persisted in the right hemisphere while M100 activation developed in the left hemisphere. When this subject was removed from the resampling pool for Experiment 2, the M50 latency difference gained significance ($p < .02$) and the M100 latency difference retained significance ($p < .005$) such that the measures of significance were approximately the same as those obtained for Experiment 1. The M100 latency differences observed in the grand average waveforms were typically present in individual subject waveforms as shown in Figure 5d.

Asymmetry in response amplitude is also evident following the M100 peak, with the magnetic field in the direction of the M100 persisting somewhat longer in the left hemisphere (Figures 5a and b). In Experiment 1, this difference was found to be significant from 98 through 167 ms with a maximum at 116 ms. In Experiment 2, this difference was found to be significant from 129 through 167 ms with a later maximum at 146 ms that slightly precedes the P2m peak. Together, these results indicate that a consistent asymmetry occurs during the rise and peak of the P2m component. The shape of the difference graphs for the two experiments suggests that there are two sources of this asymmetry, with activity peaks near 116 and 150 ms. The asymmetry during this period was accompanied by a trend toward an earlier P2m peak latency in the right hemisphere that was not found to be significant for either Experiment 1 ($p < .275$) or Experiment 2 ($p < .145$). No other significant response amplitude asymmetries were observed consistently across the two experiments during the first 300 ms.

The M50 and M100 latency differences found in the grand average data were also observed in the RMS waveforms for individual subjects (summarized in Table 1). The mean M50 and M100 latencies for subjects exhibiting bilateral peaks in their RMS waveforms were significantly earlier in the right hemisphere in Experiment 1 and exhibited a trend toward significance in Experiment 2. Bilateral M100 peaks of typical polarity and topography were identifiable in only 10 of 19 subjects in Experiment 2 as compared with 10 of 14 in Experiment 1. Some of this disparity was attributable to the smaller amplitude of the M100 component in Experiment 2.

DISCUSSION

General Characteristics of the Evoked Magnetic Field Response

The results of the present MEG study demonstrate that the grand average evoked response is remarkably consistent with respect to both surface topography and component peak latencies, despite variation both in subject anatomy and in subject head position relative to the sensors. The results are in good agreement with past EEG (Goff, et al., 1969; Picton, et al., 1974) and MEG (Hari, et al., 1987; Pantev, et al., 1991; Pelizzone, et al., 1987) studies that have collectively ascertained the components of the canonical waveform evoked in response to

auditory stimuli. In particular, the grand average data replicate the cortical waveform results previously obtained with click stimuli under EEG (Goff, et al., 1969; Picton, et al., 1974). It seems clear that the components we observed -- N_am at 18ms, P_am at 34ms, N_bm at 47ms, P1m at 58ms, and N1m at 90ms -- are the magnetic field counterparts of the electric potential components referred to as N19, P30, N40, P50, and N100. Our findings on the auditory evoked response are also consistent with previous MEG findings on gamma-band (Pantev, et al., 1991; Yoshiura, et al., 1995) and slow-wave response constituents (Pantev, et al., 1986; Lütkenhöner & Steinsträter, 1998). Specifically, the slow-wave evoked waveform exhibits a prominent deflection at ~100 ms latency, commonly referred to as the M100 or N100m, and an earlier deflection of opposite polarity, usually referred to as the M50 or P50m, which overlaps the gamma-band components.

Lateralization in the Evoked Magnetic Field Response

Our analysis of hemispheric differences in the evoked magnetic field amplitude for the two experiments identified consistent periods of significant lateralization in the slow-wave response but not in the gamma-band response. Specifically, lateralization in the slow-wave response was found during the rise of the M100 (~49–72 ms) and again during the rise and peak of the P_2m component (~129–167 ms). Significant latency lateralization was also consistently observed for the M100 component of the slow-wave response, with the M100 peaking earlier in the right hemisphere. These lateralization effects were evident not only in the grand averages but also in the majority of individual subject waveforms. These lateralization effects could reflect one or more systematic neurobiological asymmetries present in (at least) the right-handed population, or non-biological asymmetries in sensor locations or in head positioning relative to the sensors. With respect to non-biological asymmetries, the location of active sensors within the MEG helmet is not precisely symmetric, the head placement within the helmet may vary in symmetry from subject to subject, and the average head placement may be biased for a particular experiment or set of experiments. Although these non-biological asymmetries cannot be excluded as the source of our observed effects, the finding of similar rightward lateralization effects in other studies as discussed below and, more importantly, the absence of findings of leftward lateralization effects for similar stimulus conditions, suggests that non-biological asymmetries are not the primary source.

Our observations of rightward lateralization in the M100 rise amplitude and peak latency for the click stimulus are quite similar to those of König, et al. (2008) for FM sweeps (one octave in 0.5 to 4 Hz range, linear in either direction, 500 ms duration, 10 ms linear on-off ramps, presented binaurally at 0.5 Hz, 224 stimuli). This study examined magnetic field amplitude lateralization in the slow-wave response in a group of 16 right-handers using the integral of the absolute magnetic field over 20 ms windows rather than the instantaneous value of the field. The investigation found a period of significant lateralization during the M100 rise and an earlier M100 peak in the right hemisphere for both passive and task listening conditions. For the task listening condition, which is comparable to the condition used in our experiments, significant magnetic field lateralization was observed at ~60–80 ms, while the M100 peaked at 88 ms in the right hemisphere and 95 ms in the left hemisphere (7 ms latency difference significant, p=0.0024). In our study, significant lateralization was found slightly earlier, at ~49–72 ms, while the M100 peaked at nearly identical latencies, ~ 87 in the right hemisphere and ~ 96 in the left hemisphere. The slight discrepancy in the timing of the lateralization period between studies could be attributable to our use of instantaneous rather than integrated magnetic field values. Consistent with this possibility, our results showed a peak in lateralization at ~ 67 ms, late within the lateralization period, which would tend to produce a somewhat earlier period of lateralization for magnetic field values integrated over a 20 ms window.

Our results are also similar to those obtained by Hine and Debener (2007) in an EEG study that examined lateralization in the slow-wave electric potentials evoked by white noise and 1 kHz pure tones (220 ms duration, 10 ms on-off ramps, presented monaurally, ISI 1000–1400 ms, 388 repetitions) in 16 right-handed subjects. This study modeled response activity using bilateral regional source waveforms, with the tangential orientation in each hemisphere defined as the orientation of a freely rotating dipole source during the N100 onset-to-peak latency period. Tangential waveforms, which should closely correspond with evoked magnetic field waveforms, were analyzed for evidence of lateralization using methods quite similar to those we employed. Because monaural stimulation was used in this study, separate lateralization analyses were performed for waveforms generated in response to contralateral and ipsilateral stimulation. Both waveforms exhibited rightward lateralization during the rise of the N100 for both noise and tone stimuli. Furthermore, analysis of N100 peak latencies for tangential waveforms across all conditions found significantly shorter latencies in the right hemisphere. The finding of the N100 lateralization effects for *both* contralateral and ipsilateral stimulation suggests that the same effects observed for binaural stimulation do not simply reflect ear-to-hemisphere connectivity asymmetry in either direct subcortical or in interhemispheric callosal pathways.

M100 Lateralization and the Sound Energy Onset

Because essentially the same rightward lateralization of the N100 in the tangential waveform was found for tones and white noise, Hine and Debener (2007) speculated that the tangential activity might represent an early N100 component evoked by the onsets of the stimuli, which were identical 10 ms ramps. The finding of the same lateralization effects in the magnetic field waveforms evoked by 2 octave per second frequency sweeps that also contained 10 ms onset ramps (König, et al., 2008) is consistent with this hypothesis. Our discovery of the same lateralization effects in the magnetic field response to a click consisting of a 0.0625 ms square wave supports an even more general hypothesis: namely, that the early part of the M100 component reflects an asymmetric response to a sharp sound energy onset.

Further evidence that the M100 latency lateralization effect is related to relatively sharp sound energy onsets is provided in a study that examined the evoked magnetic field response in 7 right-handed subjects to amplitude and frequency modulation (AM and FM) embedded in a 667 Hz pure tone (Pardo, et al., 1999). The stimuli were binaural, 620 ms in length presented at 0.5 Hz, and included a linear doubling of frequency or amplitude incorporated at either 0 ms (onset) or 300 ms (transition). The modulation took place over 300, 30, or 3 ms intervals, which correspond to increasingly sharp onsets or transitions. The rise time for stimuli that did not incorporate an AM onset was 20 ms. The study observed M100 peak latencies for both onsets and transitions that were earlier in the right hemisphere by 1 to 11 ms for most stimuli (not significant for any onset stimulus). However, for 300 ms AM stimuli, the M100 peaked earlier in the *left* hemisphere with the difference reaching significance in the case of the AM transition ($p<0.002$). This lateralization reversal was not observed for 300 ms FM transitions suggesting that earlier M100 peaks in the right hemisphere are associated with onsets of sound energy at quiescent spectral frequencies. Thus, all of the FM stimuli and the sharp (3 and 30 ms) AM stimuli may have onset/transition spectra that are sufficiently wide-band to produce earlier M100 peaks in the right hemisphere while the 300 ms AM stimuli do not.

The results of an investigation into the M100 response for syllables starting with stop and no-stop consonants (binaural, 500 ms duration) also points to a relationship between onset dynamics and M100 latency lateralization (Gage, et al., 1998). This study, employing 5 strongly right-handed subjects, found that the M100 peak was ~15 ms earlier in the right hemisphere for syllables starting with stop consonants ($p = 0.02$) but tended to be earlier in the left

hemisphere for syllables starting with no-stop consonants ($p = 0.1$). The two types of stimuli differ in their onset dynamics, with stops having the greater sound energy onset.

Our study, as well as those described above, employed only right-handed subjects. Therefore, it is possible that the M100 lateralization effects observed in these studies is related to right-handedness. Evidence of a possible link between the M100 lateralization effects and handedness is presented in a study that examined the neuromagnetic response to tones and Finnish vowels (250 ms in length, 20 ms rise and fall times) in 27 subjects that included approximately equal numbers of right- and left-handers (Kirveskari, et al., 2006). This study found earlier M100 peak latencies in the right hemisphere for both types of stimuli; however, the effect was significant only in the group of strong right-handers (10 of 27).

Several MEG studies, in addition to those just described, have observed earlier M100 peaks in the right hemisphere for a variety of stimuli. These studies are summarized in Table 2. The results are consistent with the hypothesis that the M100 latency lateralization effect reflects asymmetry in the response to sharp sound energy onsets.

As noted, reversed M100 latency lateralization was observed for stimuli with gradual sound energy onsets (300 ms rise times) in the Pardo et al. study (1999). This was attributable to a systematic increase in M100 latency with increasing stimulus rise times that appeared to be more pronounced in the right hemisphere. Several other studies have provided evidence that M100 latency increases and amplitude decreases as sound onset rise time increases (Kondera, et al., 1979; Onishi & Davis, 1968; Biermann & Heil, 2000), but none have investigated hemispheric differences in these effects. Further investigation is required to determine if, in fact, the influence of sound energy rise time on the M100 response is more robust in the right hemisphere, as suggested by the Pardo et al. (1999) results.

M100 Peak Latency Lateralization

Lateralization in M100 peak latency is sometimes interpreted as reflecting a difference in the speed of the response to particular stimuli in the two hemispheres, with an earlier peak signifying a faster response. This interpretation would lead to the conclusion that processing proceeds more rapidly in the right hemisphere for a wide variety of stimuli, including certain speech elements such as syllables starting with a stop consonant. However, hemispheric asymmetry in myelination has been found that would potentially enhance the speed of processing in the left auditory cortex (Anderson, et al., 1999; Sigalovsky, et al., 2006). Moreover, some investigators have speculated that faster auditory processing in the left hemisphere attributable to this anatomical asymmetry (Schönwiesner, et al., 2005; Zatorre & Belin, 2001) underlies left hemisphere specialization for processing rapidly successive auditory sequences and rapidly changing acoustic information (Tallal, et al., 1993; Poeppel, 2001, 2003; Zatorre & Gandour, 2008; Zatorre, et al., 2002). Thus, the interpretation of M100 peak latency differences in terms of lateralization in the speed of response presents something of a paradox. Furthermore, this interpretation is inconsistent with certain aspects of our findings. Specifically, we found no significant latency lateralization in the pre-M100 middle latency or in the post-M100 slow-wave response components as might be expected if processing of the stimulus was proceeding more quickly in the right hemisphere. This leads us to consider an alternative hypothesis, namely, that the observed M100 lateralization effects, including the peak latency difference, reflect asymmetry in the field strength of one or more sources active during the M100 rise.

Both late M50 and early M100 activity appears to occur during the rise of the M100 and, therefore, could contribute to the observed lateralization (Inui, et al., 2006; Liégeois-Chauvel, et al., 1994; Moran, et al., 1993; Yvert, at al., 2001; Yvert, at al., 2005). Our analysis suggests that the lateralization is attributable primarily to one or more sources that peak around 67 ms.

Evidence of a late M50 source located in antero-lateral Heschl's gyrus (HG) that peaks at approximately 74 ms has been found in EEG and MEG scalp recordings (Yvert, at al., 2001). In addition, intracerebral recordings have provided evidence of an activity complex originating in antero-lateral HG that includes late M50 activity peaking at about 70 ms and late M100 activity peaking at about 120 ms (Liégeois-Chauvel, et al., 1994). Leftward asymmetry in this complex is consistent with the lateralization observed in the evoked response preceding and following the M100 peak and may well be a contributing factor to lateralization during the M100 rise. Nevertheless, the more frequently-reported finding of an early latency M100 source that peaks in the 60 to 76 ms timeframe suggests that lateralization during the M100 rise is likely to involve, if not exclusively arise from, M100-related activity (Godey, et al., 2001; Inui, et al., 2006; Liégeois-Chauvel, et al., 1994; Nätään & Picton, 1987; Woods, 1995; Yvert, at al., 2005). Recent studies indicate that this early M100 activity originates in an area located on, or slightly posterior to, medial HG (Godey, et al., 2001; Inui, et al., 2006;Yvert, at al., 2005). The potential for asymmetry in the amplitude of the magnetic field response of an early latency M100 source to produce the lateralization in M100 amplitude and latency observed in this study is demonstrated by the multiple-source, linear- summation model illustrated in Figure 6.

The posterior-to-anterior shift detected in the M100 topography is an effect that has been consistently observed in MEG studies (Lütkenhöner & Steinsträter, 1998; Rogers, et al., 1990; Rosburg, et al., 2002; Teale, et al., 1998; Zouridakis, et al., 1998). Such a shift is consistent with findings that suggest there are at least two sources within auditory cortex that contribute to the M100: an early latency source occupying a relatively posterior location, and a late latency source occupying a relatively anterior location (Loveless, et al., 1996; McEvoy, et al., 1997; Sams, et al., 1993). If the observed M100 lateralization effects involve M100-related activity and are associated with the processing of sound energy onsets as we propose, then our findings imply the existence of a very early latency M100 source located in posterior auditory cortex that responds robustly to sound energy onsets. Precisely such a source, situated near (or possibly on) Heschl's gyrus in a relatively medial-posterior position, has been identified in a recent study that employed depth electrode recordings to examine the response to the onset of sound energy versus the onset of pitch (Schönwiesner & Zatorre, 2008).

Amplitude Lateralization in the Early Latency M100 Source

Lateralization in the evoked magnetic field as represented in the MEG channel data could reflect functional asymmetry in the processing of the stimulus or asymmetry in the positioning of homologous cortical areas that is either unrelated, or not straightforwardly related, to function. The latter possibility was minimized in the Hine and Debener (2007) study, which examined lateralization in regional source waveforms derived using equivalent source modeling based on EEG channel data. Lateralization due to asymmetry in orientation or depth of cortical regions relative to sensors is presumably eliminated in regional source waveforms; thus, the Hine and Debener findings support the hypothesis that the effects observed in the MEG channel data reflect an actual processing asymmetry.

Although the Hine and Debener results (2007) strongly suggest that the M100 lateralization effects reflect a functional asymmetry, the possibility that they arise from an anatomical asymmetry cannot be totally excluded. The morphology and topography of HG and nearby cortical structures are highly variable between hemispheres (Fullerton & Pandya, 2007; Galaburda & Sanides, 1980; Rademacher, et al., 1993; Rademacher, et al., 2001), exhibiting systematic asymmetries that could be related to the leftward asymmetry found in HG volume (Doursaint-Pierre, et al., 2006; Penhune, et al., 1996). Specifically, the sulci immediately anterior and posterior to the first gyrus of Heschl extend further on the left, suggesting that the cortical surface found within the sulci is greater in the left hemisphere (Leonard, et al., 1998).

Consistent with this possibility is the finding of morphological asymmetry in HG characterized by a more constrained neck or peduncle connecting HG to the superior temporal gyrus in the left hemisphere (Leonard, et al., 2008). Such asymmetry could conceivably produce hemispheric differences in the position of the cortical area near posterior-medial HG generating the early M100 response to sound energy onsets such that orientation with respect to the horizontal plane is somewhat reversed in the left hemisphere. Such an anatomical asymmetry could reduce the amplitude of the early M100 magnetic field response in the left relative to the right hemisphere, even in regional source waveforms. Further research that includes MRI as well as MEG data is required in order to investigate the potential relationship between HG morphological asymmetry and the M100 lateralization effects.

Assuming that early latency M100 amplitude lateralization does reflect a processing asymmetry, the asymmetry could potentially underlie superior right hemisphere performance or greater right hemisphere involvement in several functional areas. The early latency M100 subcomponent generated in posterior auditory cortex has been linked to the gating of conscious awareness of sounds (Jääskeläinen, et al., 2004) and to the processing of sound location (Ahveninen, et al., 2006). Thus, rightward asymmetry in this component could contribute to biases in the stimulus-driven orienting of attention (Corbetta & Schulman, 2002) and spatial processing (Hausmann, et al., 2005; Zatorre & Penhune, 2001; Zatorre, et al., 2002) that favor the right hemisphere. In addition, asymmetry in the early latency M100 subcomponent could account for right hemisphere superiority in FM sweep-direction discrimination as proposed by König, et. al. (2008) and supported by their finding of an increase in early latency M100 amplitude lateralization for a direction discrimination over a passive listening condition. Although the computational processes comprising the above-mentioned functions are unknown, the involvement of sound energy onset processing seems likely, suggesting that a relationship between asymmetry in onset processing and lateralization in these functions is at least plausible. Lastly, M100 lateralization effects might reflect a greater influence of the dynamics of sound energy onsets in the right hemisphere response, resulting in more robust tracking of the stimulus envelope in the right hemisphere.

Acknowledgments

We are grateful to J. Walker for excellent technical assistance. This work was supported by the National Institute of Deafness and Other Communication Disorders of the National Institutes of Health through Training Grant DC-00046 to M. Howard and Grant 2R01DC05660 to D. Poeppel.

Abbreviations

AM
: Amplitude-modulated

CALM
: Continuously adjusted least squares method

FM
: Frequency-modulated

MEG
: HG, Heschl’s gyrus

LH
: Left hemisphere; Magnetoencephalography

MRI
: Magnetic resonance imaging

RH
Right hemisphere

RMS
Root-mean-square

SPL
Sound pressure level

SQUID
Superconducting quantum interference device

TSPCA
Time-shift principle component analysis algorithm

References

Adachi Y, Shimogawara M, Higuchi M, Haruta Y, Ochiai M. Reduction of nonperiodic environmental magnetic noise in MEG measurement by continuously adjusted by least square method. IEEE Trans Appl Superconduct 2001;11:669–672.

Ahveninen J, Jääskeläinen IP, Raij T, Bonmassar G, Devore S, Hämäläinen M, Levänen S, Lin FH, Sams M, Shinn-Cunningham BG, Witzel T, Belliveau JW. Task-modulated "what" and "where" pathways in human auditory cortex. Proc Natl Acad Sci USA 2006;103:14608–14613. [PubMed: 16983092]

Anderson B, Southern BD, Powers RE. Anatomic asymmetries of the posterior superior temporal lobes: A postmortem study. Neuropsychiatry Neuropsychol Behav Neurol 1999;12:247–254. [PubMed: 10527109]

Biermann S, Heil P. Parallels between timing of onset responses in single neurons in cat and of evoked magnetic fields in human auditory cortex. J Neurophysiol 2000;84:2426–2439. [PubMed: 11067985]

Corbetta M, Schulman GL. Control of goal-directed and stimulus-driven attention in the brain. Nat Rev Neurosci 2002;3:201–215. [PubMed: 11994752]

de Cheveigne' A, Simon JZ. Denoising based on time-shift PCA. J Neurosci Methods 2007;165:297–305. [PubMed: 17624443]

Doursaint-Pierre R, Penhune VB, Watkins KE, Neelin R, Lerch JP, Bouffard M, Zatorre RJ. Asymmetries of the planum temporale and Heschl's gyrus: Relationship to language lateralization. Brain 2006;129:1164–1176. [PubMed: 16537567]

Efron, B.; Tibshirani, RJ. An Introduction to the Bootstrap. Chapman & Hall; New York: 1993.

Eggermont JJ, Ponton CW. The neurophysiology of auditory perception: From single units to evoked potentials. Audiol Neurootol 2002;7:71–89. [PubMed: 12006736]

Fullerton BC, Pandya DN. Architectonic analysis of the auditory-related areas of the superior temporal region of the human brain. J Comp Neurol 2007;504:470–498. [PubMed: 17701981]

Gabriel D, Veuillet E, Ragot R, Schwartz D, Ducorps A, Norena A, Durrant JD, Bonmartin A, Cotton F, Collet L. Effect of stimulus frequency and stimulation site on the N1m response of the human auditory cortex. Hear Res 2004;197:55–64. [PubMed: 15504604]

Gage N, Poeppel D, Roberts TPL, Hickok G. Auditory evoked M100 reflects onset acoustics of speech sounds. Brain Res 1998;814:236–239. [PubMed: 9838140]

Gage N, Roberts TPL, Hickok G. Hemispheric asymmetries in auditory evoked neuromagnetic fields in response to place of articulation contrasts. Cog Brain Res 2002;14:303–306.

Galaburda A, Sanides F. Cytoarchitectonic organization of the human auditory cortex. J Comp Neurol 1980;190:597–610. [PubMed: 6771305]

Godey B, Scwartz D, deGraaf JB, Chauvel P, Liégeois-Chauvel C. Neuromagnetic source localization of auditory evoked fields and intracerebral evoked potentials: A comparison of data in the same patients. Clin Neurophysiol 2001;112:1850–1859. [PubMed: 11595143]

Goff, WR.; Matsumiya, Y.; Allison, T.; Goff, GD. Cross-modality comparisons of average evoked potentials. In: Donchin, E.; Lindsley, DB., editors. Average Evoked Potentials: Methods, Results, and Evaluations. NASA; Wash. DC: 1969. p. 95-141.

Hari R, Pelizzone M, Mäkelä JP, Hällström J, Leinonen L, Lounasmaa OV. Neuromagnetic responses of the human auditory cortex to on- and offsets of noise bursts. Audiology 1987;26:31–43. [PubMed: 3593099]

Hausmann M, Corballis MC, Fabri M, Paggi A, Lewald J. Sound lateralization in subjects with callostomy, callosal agenesis, and hemispherectomy. Cogn Brain Res 2005;25:537–546.

Hine J, Debener S. Late auditory evoked potentials asymmetry revisited. Clin Neurophysiol 2007;118:1274–1285. [PubMed: 17462945]

Huotilainen M, Winkler I, Alho K, Escera C, Virtanen J, Ilmoniemi RJ, Jääskeläinen IP, Pekkonen E, Näätänen R. Combined mapping of human auditory EEG and MEG responses. Electroencephalogr Clin Neurophysiol 1998;108:370–379. [PubMed: 9714379]

Inui K, Okamota KM, Gunji A, Kakigi R. Serial and parallel processing in the human auditory cortex: A magnetoencephalographic study. Cereb Cortex 2006;16:18–30. [PubMed: 15800024]

Jääskeläinen IP, Ahveninen J, Bonmassar G, Dale AM, Ilmoniemi RJ, Levänen S, Lin FH, May P, Melcher J, Stufflebeam S, Tiitinen H, Belliveau JW. Human posterior auditory cortex gates novel sounds to consciouness. Proc Natl Acad Sci USA 2004;101:6809–6814. [PubMed: 15096618]

Jin CY, Ozaki I, Suzuki Y, Baba M, Hashimoto I. Hemispheric asymmetry in N100m current sources in auditory evoked fields: Comparison of ipsilateral versus contralateral responses. Int Congr Ser 2007;1300:61–64.

Kanno A, Nakasoto N, Murayama N, Yoshimoto T. Middle and long latency peak sources in auditory evoked magnetic fields for tone bursts in humans. Neurosci Lett 2000;293:187–190. [PubMed: 11036192]

Kirveskari E, Salmelin R, Hari R. Neuromagnetic responses to vowels vs. tones reveal hemispheric lateralization. Clin Neurophysiol 2006;117:643–648. [PubMed: 16403672]

Kondera K, Hink RF, Yamada O, Suzuki JI. Effects of rise time on simultaneously recorded auditory-evoked potentials from the early, middle, and late ranges. Int J Audiol 1979;18:395–402.

König R, Sielu ycki C, Simserides C, Heil P, Scheich H. Effects of the task of categorizing FM direction on auditory evoked magnetic fields in the human auditory cortex. Brain Res 2008;1220:102–117. [PubMed: 18420183]

Leonard CM, Puranik C, Kuldau JM, Lombardino LJ. Normal variation in the frequency and location of human auditory cortex landmarks. Heschl's gyrus: Where is it? Cereb Cortex 1998;8:397–406. [PubMed: 9722083]

Leonard, CM.; Towler, SD.; Welcome, S.; Halderman, LK.; Otto, R.; Chiarello, C. Neuroscience. Wash. D.C: Society for Neuroscience; 2008 Nov. Lateral asymmetry in the shape of Heschl's gyrus; p. 15-19.

Liégeois-Chauvel C, Musolino A, Badier JM, Marquis P, Chauvel P. Evoked potentials recorded from the auditory cortex in man: Evaluation and topography of the middle latency components. Electroencephalogr Clin Neurophysiol 1994;92:204–214. [PubMed: 7514990]

Loveless N. Temporal integration in auditory sensory memory: Neuromagnetic evidence. Electroencephalogr Clin Neurophysiol 1996;100:220–228. [PubMed: 8681863]

Lütkenhöner B, Steinsträter O. High-precision neuromagnetic study of the functional organization of the human auditory cortex. Audiol Neurootol 1998;3:191–213. [PubMed: 9575385]

McEvoy L, Levänen S, Loveless N. Temporal characteristics of auditory sensory memory: Neuromagnetic evidence. Psychopysiology 1997;34:308–316.

Moran JE, Tepley N, Jacobsen GP, Barkley GL. Evidence for multiple generators in evoked responses using finite difference field mapping: Auditory evoked fields. Brain Topogr 1993;5:229–240. [PubMed: 8507549]

Näätänen R, Picton T. The N1 wave of the human electric and magnetic response to sound: A review and an analysis of the component structure. Psychopysiology 1987;24:375–425.

Obleser J, Lahiri A, Eulitz C. Auditory-evoked magnetic field codes place of articulation in timing and topography around 100 milliseconds post syllable onset. Neuroimage 2003;20:1839–1847. [PubMed: 14642493]

Oldfield RC. The assessment and analysis of handedness: The Edinburgh inventory. Neuropsychologia 1971;9:97–113. [PubMed: 5146491]

Onishi J, Davis H. Effects of duration and rise time of tone bursts on evoked V potentials. J Acoust Soc Am 1968;44:582–591. [PubMed: 5665530]

Pantev C, Makeig S, Hoke M, Galambos R, Hampson S, Gallen C. Human auditory evoked gamma-band fields. Proc Natl Acad Sci USA 1991;88:8996–9000. [PubMed: 1924362]

Pantev C, Lütkenhöner B, Hoke M, Lehnertz K. Comparison between simultaneously recorded auditory-evoked magnetic fields and potentials elicited by ipsilateral, contralateral and binaural tone burst stimulation. Audiology 1986;25:54–61. [PubMed: 3954684]

Pardo PJ, Mäkelä JP, Sams M. Hemispheric differences in processing tone frequency and amplitude modulations. NeuroReport 1999;10:3018–3086.

Pelizzone M, Hari R, Mäkelä JP, Huttunen J, Ahlfors S, Hämäläinen M. Cortical origin of middle-latency auditory evoked responses in man. Neurosci Lett 1987;82:303–307. [PubMed: 3696502]

Penhune VB, Zatorre RJ, MacDonald JD, Evans AC. Interhemispheric anatomical differences in human primary auditory cortex: Probabilistic mapping and volume measurement from magnetic resonance scans. Cereb Cortex 1996;6:661–672. [PubMed: 8921202]

Picton TW, Hillyard SA, Krausz HI, Galambos R. Human auditory evoked potentials. I Evaluation of components Electroencephalogr. Clin Neurophysiol 1974;36:179–190.

Poeppel D. Pure word deafness and the bilateral processing of the speech code. Cogn Sci 2001;21:679–693.

Poeppel D. The analysis of speech in different temporal integration windows: Cerebral lateralization as ‘asymmetric sampling in time’. Speech Commun 2003;41:245–255.

Poeppel D, Phillips C, Yellin E, Rowley HA, Roberts TPL, Marantz A. Processing of vowels in supratemporal auditory cortex. Neurosci Lett 1997;221:145–148. [PubMed: 9121685]

Rademacher J, Caviness VS, Steinmetz H, Galaburda AM. Topological variation of the human primary cortices: Implications for neuroimaging, brain mapping, and neurobiology. Cereb Cortex 1993;3:313–329. [PubMed: 8400809]

Rademacher J, Morosan P, Schormann T, Schleicher A, Werner C, Freund HJ, Zilles K. Probablistic mapping and volume measurement of human primary auditory cortex. Neuroimage 2001;13:669–683. [PubMed: 11305896]

Roberts TPL, Ferrari P, Stufflebeam SM, Poeppel D. Latency of the auditory evoked neuromagnetic field components: Stimulus dependence and insights toward perception. J Clin Neurophysiol 2000;17:114–129. [PubMed: 10831104]

Rogers RL, Papanicolaou AC, Baumann SB, Saydjari C, Eisenberg HM. Neuromagnetic evidence of a dynamic excitation pattern generating the N100 auditory response. Electroencephalogr Clin Neurophysiol 1990;77:237–240. [PubMed: 1691977]

Rosburg T, Haueisen J, Sauer H. Habituation of the auditory evoked field component N100m and its dependence on stimulus duration. Clin Neurophysiol 2002;113:421–428. [PubMed: 11897542]

Salajegheh A, Link A, Elster C, Burghoff M, Sander T, Trahms L, Poeppel D. Systematic latency variation of the auditory evoked M100: From average to single-trial data. Neuroimage 2004;23:288–295. [PubMed: 15325376]

Sams M, Hari R, Rif J, Knuutila J. The human memory auditory trace persists about 10 sec: Neuromagnetic evidence. J Cognit Neurosci 1993;5:363–370.

Schönwiesner M, Rübsamen R, von Cramon DY. Hemispheric asymmetry for spectral and temporal processing in the human antero-lateral auditory belt cortex. Eur J Neurosci 2005;22:1521–1528. [PubMed: 16190905]

Schönwiesner M, Zatorre RJ. Depth electrode recordings show double dissociation between pitch processing in lateral Heschl’s gyrus and sound onset processing in medial Heschl’s gyrus. Exp Brain Res 2008;187:97–105. [PubMed: 18236034]

Sigalovsky IS, Fischl B, Melcher JR. Mapping an intrinsic MR property of gray matter in auditory cortex of living humans: A possible marker for primary cortex and hemispheric differences. Neuroimage 2006;32:1524–1537. [PubMed: 16806989]

Tallal P, Miller S, Fitch R. Neurobiology of speech: A case for the preeminence of temporal processing. Ann NY Acad Sci 1993;682:27–47. [PubMed: 7686725]

Teale P, Sheeder J, Rojas DC, Walker J, Reite M. Sequential source of the M100 exhibits inter-hemispheric asymmetry. Neuroreport 1998;9:2647–2652. [PubMed: 9721949]

Woods DL. The component structure of the N1 wave of the human auditory evoked potential. Electroencephalogr Clin Neurophysiol Suppl 1995;44:102–109. [PubMed: 7649012]

Yoshiura T, Ueno S, Iramina K, Masuda K. Source localization of middle latency auditory evoked magnetic fields. Brain Res 1995;703:139–144. [PubMed: 8719625]

Yvert B, Crouzeix A, Bertrand O, Seither-Preisler A, Pantev C. Multiple supratemporal sources of magnetic and electric auditory evoked potentials middle latency components in humans. Cereb Cortex 2001;11:411–423. [PubMed: 11313293]

Yvert B, Fischer C, Bertrand O, Pernier J. Localization of human supratemporal auditory areas from intracerebral auditory evoked potentials using distributed source models. Neuroimage 2005;28:140–153. [PubMed: 16039144]

Zatorre RJ, Belin P. Spectral and temporal processing in the human auditory cortex. Cereb Cortex 2001;11:946–953. [PubMed: 11549617]

Zatorre RJ, Belin P, Penhune V. Structure and function of auditory cortex: Music and speech. Trends Cog Sci 2002;6:37–46.

Zatorre RJ, Bouffard M, Ahad P, Belin P. Where is the “where” in the human auditory cortex? Nat Neurosci 2002;5:905–909. [PubMed: 12195426]

Zatorre RJ, Gandour JT. Neural specializations for speech and pitch: Moving beyond the dichotomies. Phil Trans R Soc B 2008;363:1087–1104. [PubMed: 17890188]

Zatorre RJ, Penhune VB. Spatial localization after incision of human auditory cortex. J Neurosci 2001;21:6321–6328. [PubMed: 11487655]

Zouridakis G, Simos PG, Papanicolaou AC. Multiple bilaterally asymmetric cortical sources account for the auditory N1m component. Brain Topogr 1998;10:183–189. [PubMed: 9562539]

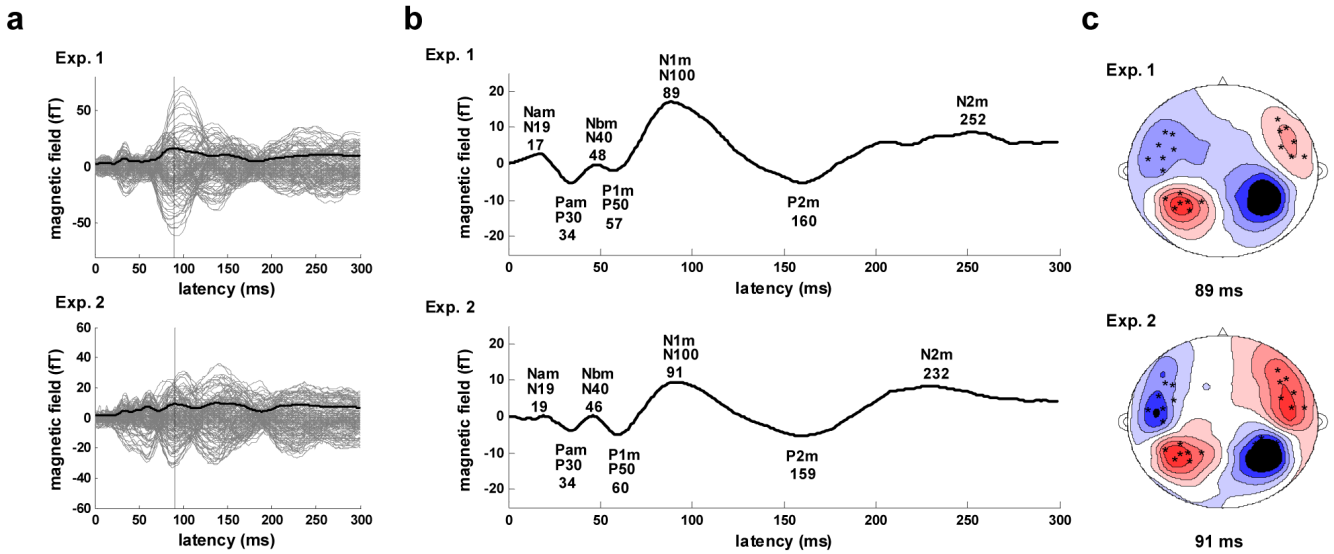

Figure 1.

Whole-head response. a) Evoked response for Experiment 1 (upper) and 2 (lower). Response for all 157 channels (gray), RMS waveform averaged across the 157 channels (solid black), N1m peak in RMS waveform (vertical black). b) Evoked response waveforms (average across all 157 channels). Major components are labeled and latencies of component peaks (ms) are shown below labels. c) Contour map of the evoked magnetic field at N1m peak latency. Sources are shown in red, sinks in blue, and the 28 channels (seven in each quadrant) with the strongest response are indicated by black × marks. This pattern is the canonical topography for auditory evoked fields at the M100 peak and reflects the separate (left versus right) underlying dipoles generating this field pattern.

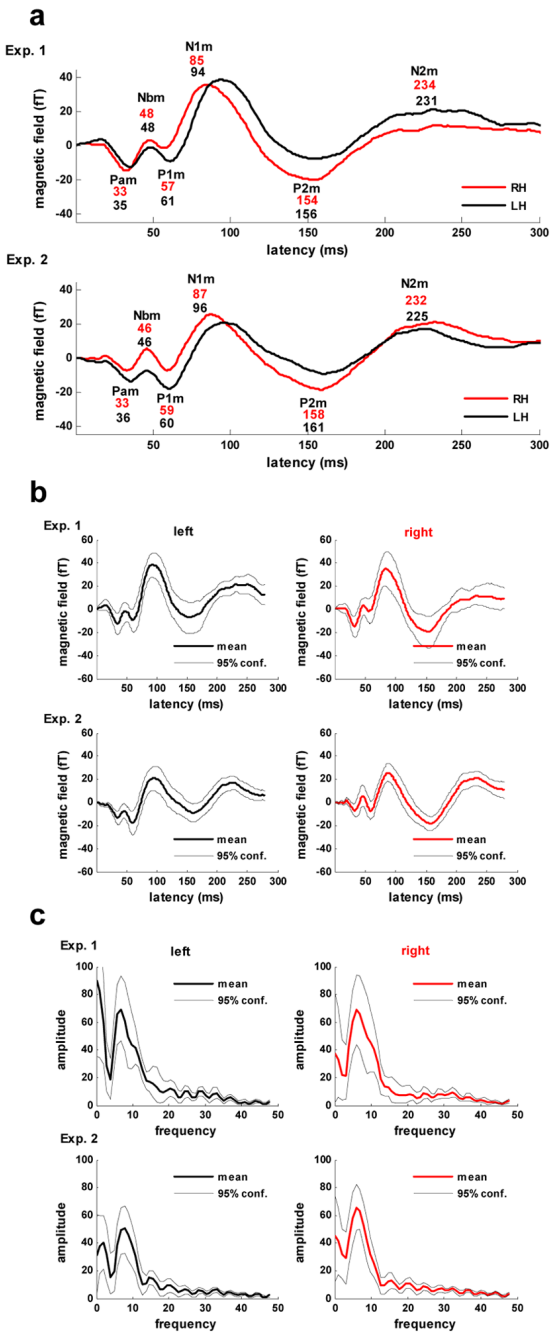

Figure 2.

Hemispheric responses. a) The evoked response waveforms for the right (RH) and left (LH) hemispheres obtained by averaging over each hemisphere's channels within the select 28 channel set. Major components are labeled and latencies of component peaks (ms) for the right (upper value, red) and left (lower value, blue) hemispheres are shown below labels. b) Bootstrap resampling results for evoked response waveforms in the right and left hemispheres. c) Frequency spectrum analysis of the bootstrap resampled waveforms for the right and left hemispheres.

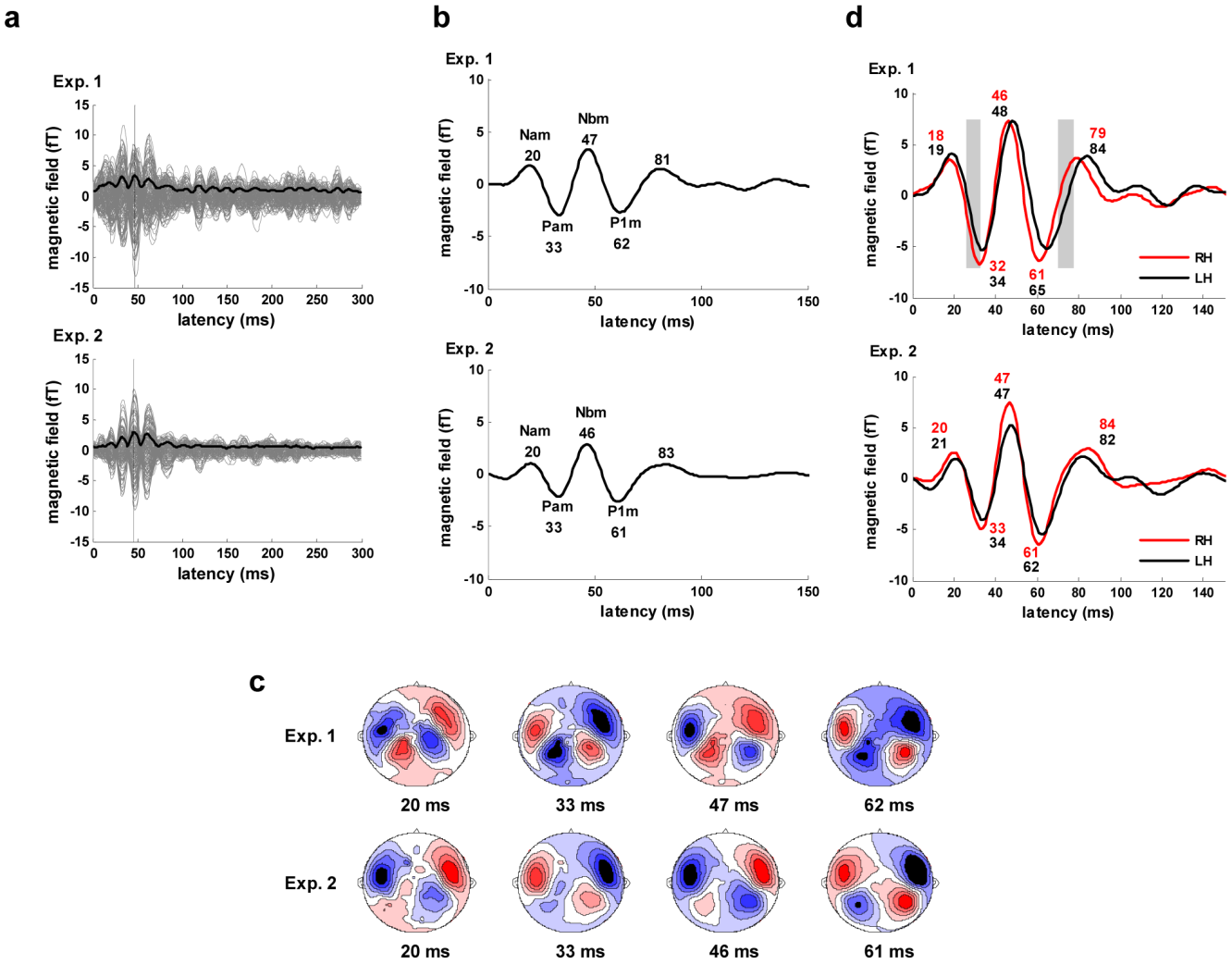

Figure 3.

Gamma band (22–58 Hz) response. a) Evoked response for Experiment 1 (upper) and 2 (lower). Response for all 157 channels (gray), whole-head RMS waveform averaged across all 157 channels (solid black), N1m peak in RMS waveform (vertical black). b) Whole-head evoked response waveforms (average across all 157 channels). Major components are labeled and latencies of component peaks (ms) are shown below labels. c) Contour maps of the evoked magnetic field at the major component peak latency times for Experiment 1 (upper) and 2 (lower). Sources shown in red, sinks in blue. d) Evoked response waveforms for the right (RH) and left (LH) hemispheres obtained by averaging over each hemisphere's channels within the select 28 channel set. Major components are labeled and latencies of component peaks (ms) for the right (upper value, red) and left (lower value, blue) hemispheres are shown below labels. Areas of significant difference in response amplitude are indicated by gray blocks.

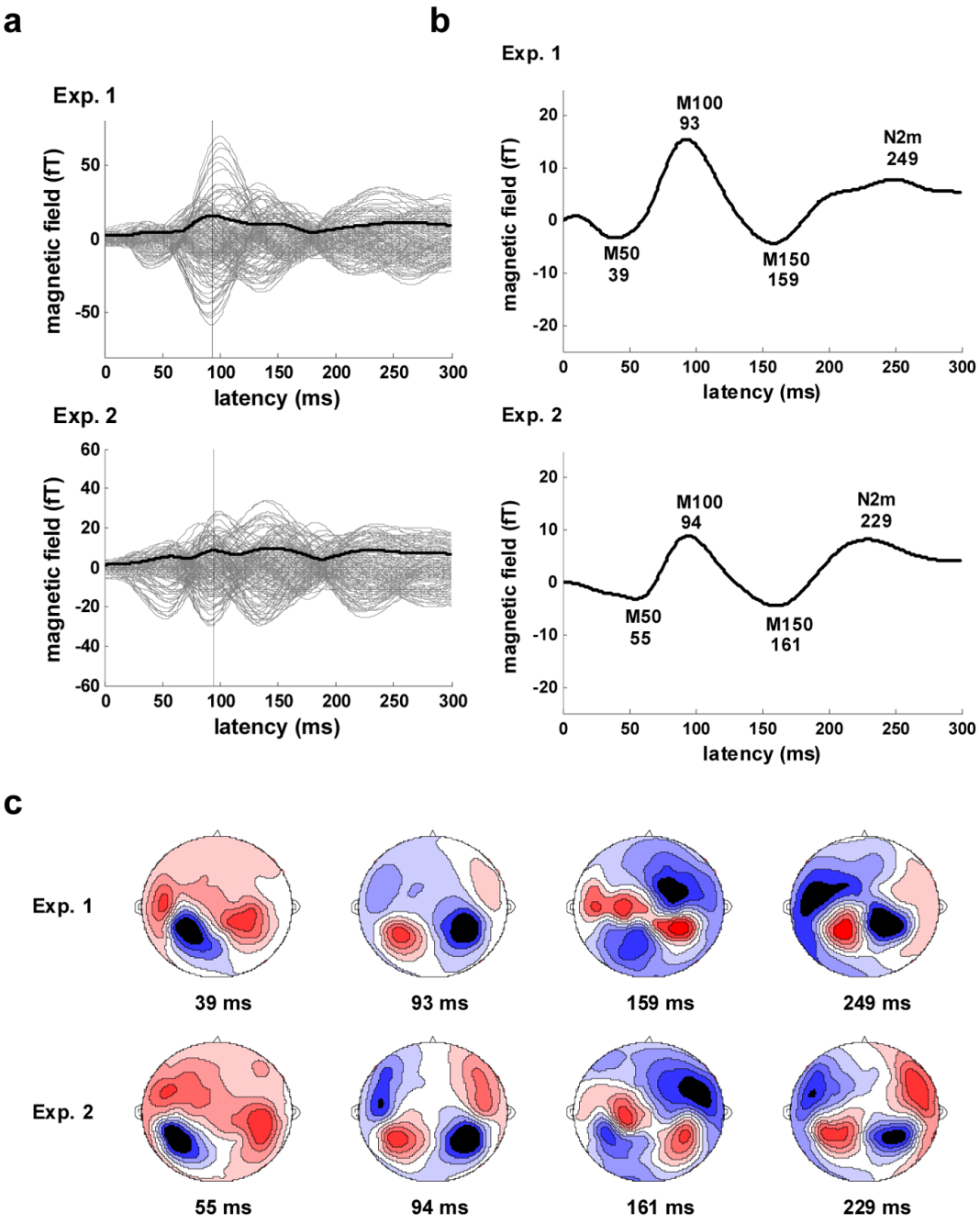

Figure 4.

Slow wave (<22 Hz) response. a) Evoked response for Experiment 1 (upper) and 2 (lower). Response for all 157 channels (gray), whole-head RMS waveform averaged across all 157 channels (solid black), N1m peak in RMS waveform (vertical black). b) Whole-head evoked response waveforms (average across all 157 channels). Major components are labeled and latencies of component peaks (ms) are shown below labels. c) Contour maps of the evoked magnetic field at the major component peak latencies for Experiment 1 (upper) and 2 (lower). Sources shown in red, sinks in blue.

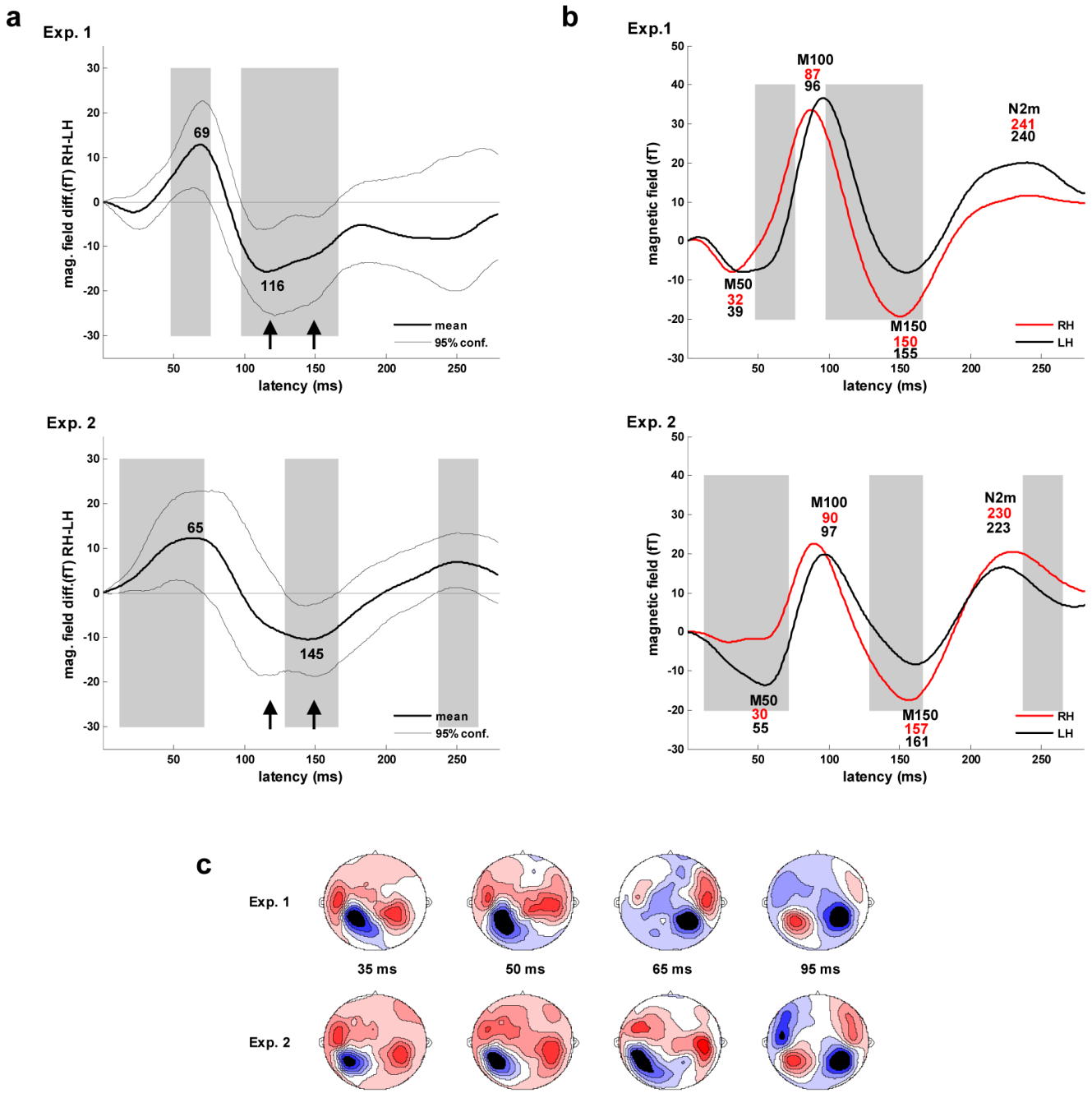

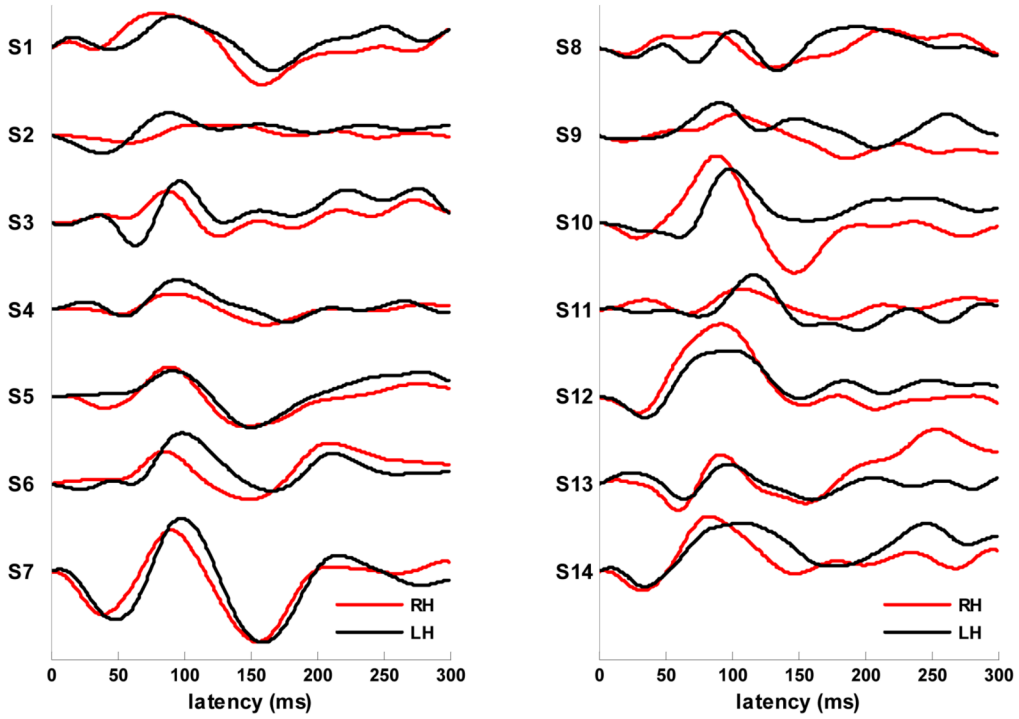

Figure 5.

Asymmetry in the evoked response. a) Difference waves computed as RH (right hemisphere) amplitude - LH (left hemisphere) amplitude using the slow-wave (<22 Hz) response amplitudes shown in 5b. Areas of significant difference in response amplitude are indicated by gray blocks. The latency of the points of maximal lateralization (ms) are shown in black. Points of increased lateralization following the M100 peak are marked with arrows. b) Waveforms for the slow-wave (<22 Hz) response in the right (RH) and left (LH) hemispheres obtained by averaging over each hemisphere's channels within the select 28 channel set. Major components are labeled and latencies of component peaks (ms) for the right (upper value, red) and left (lower value, blue) hemispheres are shown below labels. Areas of significant difference in response amplitude are indicated by gray blocks. c) Contour maps of the evoked magnetic field at 35, 50 and 65 ms show the transition from M50 to M100 dipole activation for Experiment 1 (upper) and 2 (lower). M50 topography persists in the left hemisphere while the right hemisphere transitions to M100 topography. Contour maps at 65 and 95 ms shown the posterior-to- anterior shift in the M100 activity in the right hemisphere. Sources are shown in red, sinks in blue. d) Individual subject waveforms (all 14 subjects from experiment 1) for the slow-wave (<22 Hz) response in the right (RH) and left (LH) hemispheres obtained by averaging over each hemisphere's channels within the select 28 channel set.

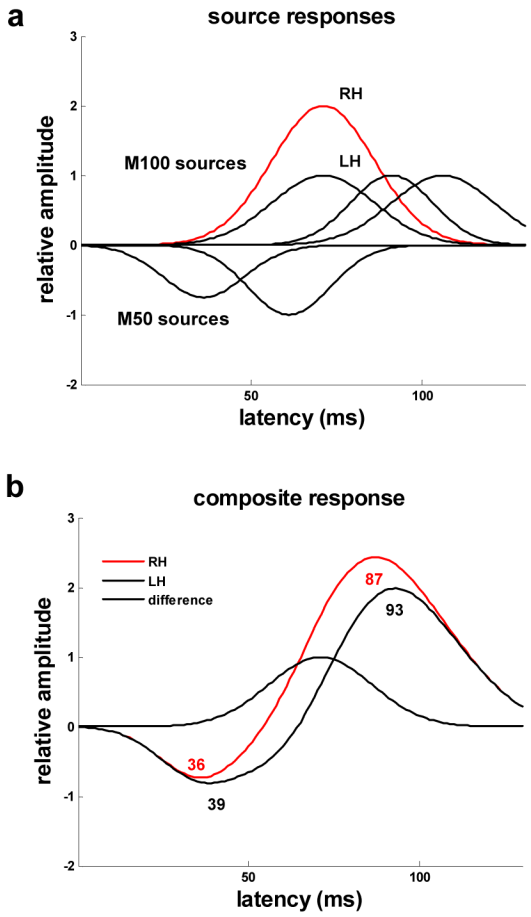

Figure 6.

A multi-source model of the M50-M100 evoked response. a) Gaussian distributions around source peak latencies model the magnetic field amplitude of two M50 sources and three M100 sources as a function of time. Amplitudes for the earliest latency M100 source differ for the right (RH-red) and left (LH-blue) hemispheres. b) For the composite response, computed as the linear sum of the magnetic field amplitudes for the five sources, the M100 component peaks earlier in the right hemisphere and the M100 rise is right-lateralized with maximum amplitude lateralization occurring at the early M100 source activity peak.

Table 1

Peak latencies from subject RMS data

	n	Latency (ms)		ANOVA		
	Bilateral (LH≥RH)	**LH**	**RH**	**df**	**F-stat**	***p***
			M50			
Ex1	11(11)	48	37	21	4.96	.038
Ex2	10(7)	52	42	19	2.88	.107
			M100			
Ex1	10(10)	94	83	19	5.61	.029
Ex2	10 (9)	95	86	19	3.70	.070

Statistics for experiments 1 and 2 where n is number of subjects with bilateral peaks in RMS waveform.

Latency values are means. Single-factor ANOVA used to determine significance of difference in means.

Table 2

Summary M100 peak latency lateralization findings

Study	Hand preference	No. of subjects	Stimuli	Presentation	Comparison	Duration (ms)	Rise (ms)	LH-RH M100 (ms)	Signif.
Gabriel, et al., 2004	right	8	tones - 1, 2, 4, 6, 8, 12 kHz	monaural	contralateral	200	3	<10	p=0.063
Gage, et al., 2002	right	7	syllables – Eng. CV stop voiced	binaural		not given	n.a.	6.6	p=0.07
Huotilainen, et al., 1998	right	8	tones - 600 Hz	binaural		200	10	3	n.s.
Jin, et al., 2007	right	33	tones - 400 Hz	monaural	contra & ipsilateral	50	2	~ 5	not given
	other	2							
Kanno, et al., 2000	right	24	tones - 2 kHz	monaural	contra & ipsilateral	60	10	~ 6–7	not given
Obleser, et al., 2003	strong right	22	syllables – Ger. CV stop voiced	binaural		350	n.a.	7	p<0.07
Poeppel, et al., 1997	right	4	vowels	monaural	contralateral	300	5	> 0	p=0.1
	left	2							
Roberts, et al., 2000	unknown	5	tones – 100 -1k Hz	monaural	contralateral	400	not given	<7	not given
Rosburg, et al., 2002	right	15	tones – 1kHz	monaural	contralateral	50, 100, 200	not given	<10	n.s.
Salajegheh, et al., 2004	right	14	tones - 125, 250, 1k Hz	binaural		400	10	5–10	not given